JOURNAL OF NANO- AND ELECTRONIC PHYSICS
Vol. **6** No 1, 01005(5pp) (2014)

ЖУРНАЛ НАНО- ТА ЕЛЕКТРОННОЇ ФІЗИКИ
Том **6** № 1, 01005(5cc) (2014)

Synthesis, Characterization and Density Functional Study of $LiMn_{1.5}Ni_{0.5}O_4$ Electrode for Lithium ion Battery

M. Aruna Bharathi[1], K. Venkateswara Rao[2], M. Sushama[1]

[1] *EEE Department, JNTUCE ,JNTU Hyderabad 500085, India*
[2] *Centre for Nano Science and Technology, IST, JNTU Hyderabad 500085, India*

(Received 31 October 2013; revised manuscript received 04 April 2014; published online 06 April 2014)

This paper analyses material issues of development of Li-ion batteries to store electrical energy. The performance of the battery is improved by developing the high energy density cathode materials at Nano level. This paper explains the synthesis of most interesting cathode material Lithium Manganese Spinel and its derivatives like transition metal oxide ($LiNi_{0.5}Mn_{1.5}O_4$) using Co-Precipitation chemical method; it is one of the eco-friendly ,effective, economic and easy preparation method. The structural features of $LiNi_{0.5}Mn_{1.5}O_4$ was characterized by XRD – analysis indicated that prepared sample mainly belong to cubic crystal form with Fd3m space group ,with lattice parameter $a = 8.265$ and average crystal size of 31.59 nm and compared the experimental results with computation details from first principle computation methods with Quantum wise Atomistix Tool Kit (ATK),Virtual Nano Lab. First principle computation methods provide important role in emerging and optimizing this electrode material. In this study we present an overview of the computation approach aimed at building $LiNi_{0.5}Mn_{1.5}O_4$ crystal as cathode for Lithium ion battery. We show each significant property can be related to the structural component in the material and can be computed from first principle. By direct comparison with experimental results, we assume to interpret that first principle computation can help to accelerate the design & development of $LiNi_{0.5}Mn_{1.5}O_4$ as cathode material of lithium ion battery for energy storage.

Keywords: Co-precipitation, DFT, Li-ion Battery, $LiNi_{0.5}Mn_{1.5}O_4$, XRD, Transmission spectrum, Band structure, Density of states.

PACS numbers: 82.47.Aa, 71.20. – b

1. INTRODUCTION

There is a current global need for storage of electrical energy. Future generations of rechargeable lithium batteries are required to power portable electronic devices, store electricity generated from renewable sources, and hybrid electric vehicle applications. Li-ion offers higher energy density, longer cycle life, and no memory effect compared to lead acid batteries. In order to develop most economic ecol-friendly and efficient battery with development of low cost material as cathode at Nano scale.

Commercially available Lithium ion batteries presently use $LiCoO_2$, $LiNiO_2$, $LiNi_yCO_{1-y}O_2$ as cathode materials in LIBs, but they are considered to be more expensive and toxic. The $LiMn_2O_4$ has been studied expansively as a cathode material for LIB because it is relatively inexpensive and echo friendly.Nano structured materials possess a huge surface area. As the particle size is reduced to Nano scale, large surface area is available hence their electrical, magnetic and chemical properties gets improved. Regarding to the electrical properties, as the surface area increases it capacity increases there by voltage and power.

Nano technology is the best tool for achieving breakthrough in Li-ion battery electrode material. In order to improve the performance of batteries it is desired to develop high energy density cathode materials using Nano materials. Lithium Manganese Spinel and its derivatives like transition metal oxide is one of the most interesting cathode materials with several advantages such as non-toxicity, stability, easy preparation, low cost material, abundance, high safety, environmental compatibility, good cycling properties and good storage capability[1].

The isotropic structure of Lithium Manganese Spinel provides a 3D network for fast Lithium insertion and desertion [2]. All Li ions are in the cathode sides initially and the battery system is assembled in "discharged" status. While charging, Li ions are extracted from the cathode host, solvate into and move through the non-aqueous electrolyte, and intercalate into the anode host. Meanwhile, electrons also move from cathode to anode through the outside current collectors forming an electric circuit. The chemical potential of Li is much higher in the anode than in the cathode, thus the electric energy is stored in the form of (electro) chemical energy. Such process is reversed when the battery is discharging where the electrochemical energy is released in the form of electric energy. The equilibrium voltage difference between the two electrodes, also referred to as the open circuit voltage depends on the difference of the Li chemical potential between the anode and cathode. $LiMn_2O_4$ is one of the materials currently used as an active cathode material in commercial batteries and has an open circuit voltage of more than 4 V with respect to metallic lithium. Such high cell voltage, typical for transition metal oxides, combined with a relatively high charge-storage capacity, highlights the potential of these materials in high-energy density rechargeable batteries [3-6]. $LiMn_2O_4$ was doped with Nickel, doping did not appear to change the basic $LiMn_2O_4$ structure but slightly change the lattice parameters due to atom size effect [7-9].

Molecular dynamics (MD) simulations were carried out to investigate the local structural disorder in $LiMn_2O_4$ spinel. Small but significant shifts of lithium and oxygen atom positions from the high symmetry sites of the Fd3m lattice were observed. The geometric structure and electronic properties of $LiM_xMn_{2-x}O_4$ (M = Ni or

Cu) surface can be studied at atomic scale through first principle calculation to allow enhanced understanding of the nature of the material surface and also studied the stability and electronic structure of the $LiMn_{1.5}Ni_{0.5}O_4$ (001) and (100) surfaces is metallic due to the contribution of surface Mn and Ni atoms[10, 11]. The (010) surface exhibits most stable termination which favors the Lithium diffusion in one dimension path way the electronic structure of $LiMn_{1.5}Ni_{0.5}O_4$, (010) surface is quite similar to that of the bulk. In this paper a computer calculations were obtained using Density functional theory. By comparing the calculation results of the band gap, conductive properties and formation of energy between the adsorption surface and bulk material will reveal the electro-chemical performance of $LiMn_2O_4$ and provide a theoretical foundation for large scale production [12].

The computer based simulations starts with the most basic properties of the elements and physical principles, therefore they can give the structural and electronic properties of the materials without the disturbance of the side-effect that could happen during the synthesis or characterization processes. However, since there are a lot of approximations in the theory and algorithm, computer-based computation can only simulate materials with periodic structures and the absolute values of the calculated results are correct only in a certain accuracy range. Therefore it is more important to compare the trend rather than the absolute value when use the computation results to explain the experimental phenomenon or predict the unknown properties. Calculation were performed using Atomistix Tool Kit simulation in Quantum Wise software based on Density functional theory the cut off energy of the plane wave was set at 500 eV in reciprocal K space[10-18].

The band structure of $LiMn_2O_4$ at the Fermi level is shown in figure 4. The band gap is 1.23 eV which is smaller than the calculated one of the bulk (2.38 eV). In terms of proposed diagram of electronic structure in $LiNi_xMn_{2-x}O_4$ during the charging Process, electrons are taken from the manganese eg level, and, after being used up, are taken from the eg level of nickel. A binding energy of electron in eg level of Mn and Ni ions are estimated to be 1.5-1.6 eV and 2.1 eV, respectively, This is accompanied by a step lowering of the Fermi level by the 0.5-0.6 eV, corresponding to the jumping the Li / $LiNi_xMn_{2-x}O_4$ cathode potential. This leads to a higher charge-discharge potential. However, the above mentioned mechanism of the increase of intercalation voltage in $LiNi_xMn_{2-x}O_4$ compared with pure $LiMn_2O_4$ is only a qualitative analysis. The structural and electrochemical features of pure spinel and doped samples with Ni and Cu separately were investigated and they belong cubic crystal form with Fd 3m space group or primitive simple cubic ($P4_332$) depends on its synthetic routes [6]. The phase central spinel is more promising to become cathode material. The Mn^{3+} and Mn^{4+} ions as well as the doping metal ions as in $LiMn_2O_4$ structure, occupy the octahedral (16d) sites and Lithium occupy tetrahedral (8A) sites and oxygen (32e) sides [7]. Doping did not appear to change the basic $LiMn_2O_4$ structure, but slightly change the lattice parameter due to atomic size effect. Comparison between experimental and theoretical data exhibit good fitting of peak positions obtained in XRD [8-11].

Table 1 – Lattice co-ordinates of spinel Li-Mn-O. Lattice constant a = 8.265 from XRD result

Atom	Site	Wyckoff positions		
		$x\backslash a$	$y\backslash b$	$z\backslash c$
Li	8a	0	0	0
Mn	16d	0.625	0.625	0.625
O	32e	0.3873	0.3873	0.3873

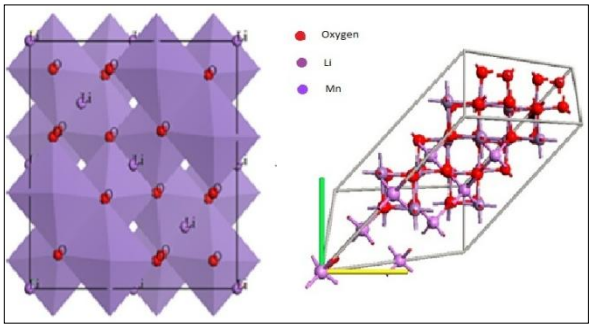

Fig. 1 – Cubic spinel with Fd3m space group $LiMn_{2-x}M_xO_4$

2. EXPERIMENTAL DETAILS

2.1 Materials Preparation

$LiMn_2O_4$ and $LiNi_{0.5}Mn_{1.5}O_4$ powders were synthesized by reacting a stoichiometric mixture of $Li(CH_3COO)\cdot 2H_2O$(AR, 99 %), $Mn(NO_3)_2$ (AR, 50 % solution), and $Ni(NO_3)_2\cdot 6H_2O$(AR, 99 %). The above chemicals were mixed at a predetermined molar ratio of Li : Mn = 1 : 2 or Li : Mn : Ni = 1 : 1.5 : 0.5, in distilled water. The pH of the mixed solution was maintained 7.5 by adding ammonium hydroxide solution [$NH_3\cdot H_2O$ (AR, 25 %) [12]. The excess water was removed by ultrasonic irradiation stirring in a home made mini ultrasonic cleaner (50 W, 28 kHz) for about 5 h at 80 °C, and the metal precipitate was formed. The metal precipitate was dried in vacuum drying oven for 12 h at 110 °C in order to dry precursors. Then the precursors were heat treated at 700 °C for 6 h at ambient condition, and then air-cooled to room temperature, yielding dark powders. After through grinding powder samples were obtained [13-16].

2.2 Structural Characterization

The crystal phases of the synthesized powder were determined by X-ray Diffraction(XRD, Bruker D8 & Advance, Germany) using Cu Kα [20-24] as variation sources (40 kV, step size 0.02, scan rate 0.5° per min in the range 2Θ = (20-80).

3. RESULTS AND DISCUSSION

3.1 X-ray diffraction

Figure shows the XRD pattern of the synthesised product all the diffraction peaks corresponding to spinel structure with space group of Fd3m [17] and diffraction data is in good conformity with the standard diffraction data of spinel compound. The average grain size of the samples was calculated using Scherer's formula as 31.59 nm, d spacing of lattice planes depends on the size of the unit cell and determines the position of the peaks [18].

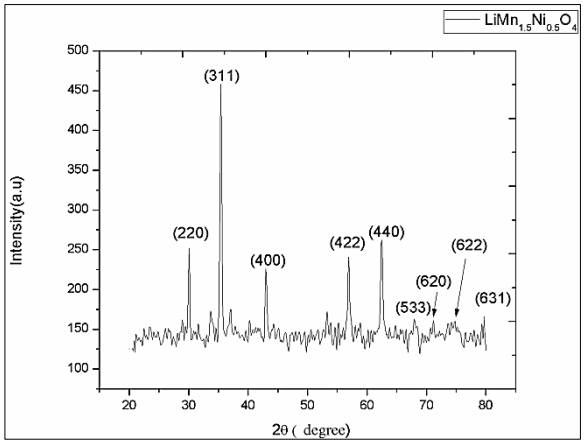

Fig. 2 – XRD pattern of Li $Mn_{1.5}Ni_{0.5}O_4$

Constructive interference of X-ray radiation occurs in a material when Bragg's law is satisfied

$$2d\sin\Theta = n\lambda$$

Where d is the distance between equivalent atomic planes, Θ is the angle between the incident beam and these planes, n is an integer and λ is wavelength.

The cubic structure of $LiMn_{1.5}Ni_{0.5}O_4$ studied in this paper facilitates the determination of the lattice parameter (a) from one diffraction peak according to:

$$\frac{1}{d} = \frac{\sqrt{h^2 + h^2 + l^2}}{a}$$

Where h, k, l are Miller indices of measured reflection. lattice parameter of $LiMn_{1.5}Ni_{0.5}O_4$ determined and is equal to a = 8.265 Å and volume = 564.665 $Å^3$.

Strain of the crystal is determined from strain equation

$$\boldsymbol{e} = \frac{\beta\cos\Theta}{4\sin\Theta}$$

and its average value is 0.002864.The line width and shape of the peaks derived from conditions of measuring particle size of the sample material. Li insertion / de-insertion and size depends up on synthesis methods $LiMn_{1.5}Ni_{0.5}O_4$ can lead to higher charge and discharge rates [19].

Table 2 – Lattice constants and size of spinel Li $Mn_{1.5}Ni_{0.5}O_4$ (Experimental Results)

Structure	Space Group	Lattice parameter(Å) LDA	Lattice parameter(Å) Experimental	Volume ($Å^3$)
Cubic	Fd3m	8.3256	8.2654	564.665

3.2 Theoretical Calculations (Results and Discussion)

First principle calculations using DFT in LDA (Local Density Approximation) approximation have demonstrated the ability to model the structural aspects of $LiMn_2O_4$. All energies were calculated with the Quantum Wise Atomistix Tool Kit (ATK) simulation package. A plane wave basis set was chosen. The results compiled in table (IV) were calculated for primitive unit cell. All energies were per formula unit. $LiMn_2O_4$ has significant stabilization energy.

Crystals are important whenever we wish to perform atomistic simulations of large or infinite system. The conventional unit cell of $LiMn_2O_4$ has 56 atoms (Li-8, Mn-16,O-32). To speed up our calculations we have used the primitive unit cell. Free energies [23] of chemical reactions were calculated and show in table (IV).

3.3 Device Configuration

In ATK, a device configuration is a way of representing the atomic structure of two semi-infinite electrodes and some different structure between them. By using VNL in ATK device $LiMn_{1.5}Ni_{0.5}O_4$ was constructed. The device geometry constructed in builder was sent to script generator and optimized, then calculation and analysis of transmission spectrum were performed. To speed up calculation, set density mesh cut-off and energy range was adjusted, self-energy calculation to Krylov (fastest method). Script was sent to job manager to compute transportation calculations and repeat it for various bias voltages. Transmission spectrum results were visualized as shown in fig. 3. I-V curve of a device was obtained with current as a function of bias voltage. At different bias I-V curve and conductance were obtained as shown in fig. 4 and 5. Device density of states and total energy were also computed. First principle calculations offer an excellent way to predict the Li intercalation voltage in metal oxides. The predictive capabilities of this technique create a unique way to design new battery materials [20-22].

Table 3 – Selected lattice coordinate inside unit cell of spinel $LiMn_{1.5}Ni_{0.5}O_4$

Atoms	Lattice coordinates		
	X(Å)	Y(Å)	Z(Å)
Lithium	0	0	0
Lithium	2.065	2.065	2.065
Oxygen	3.199098	3.199098	3.199098
Oxygen	5.060902	5.060902	3.199098
Oxygen	5.060902	3.199098	5.060902
Oxygen	3.199098	5.060902	5.060902
Oxygen	5.264098	5.264098	7.125902
Oxygen	7.125902	7.125902	7.125902
Oxygen	5.264098	7.125902	5.264098
Oxygen	7.125902	5.264098	5.264098
Manganese	5.1625	5.1625	5.1625
Manganese	3.0975	3.0975	5.1625
Nickel	3.0975	5.1625	3.0975
Nickel	5.1625	3.0975	3.0975

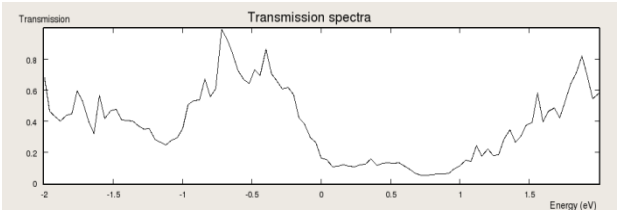

Fig. 3 – Transmission Spectrum of device $LiMn_{1.5}Ni_{0.5}O_4$

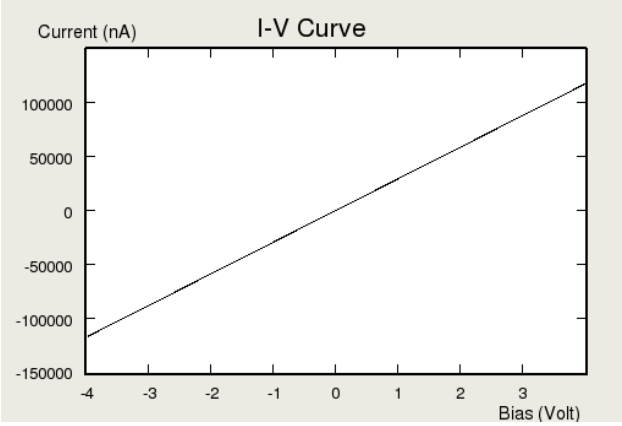

Fig. 4 – I-V charecteristic $LiMn_{1.5}Ni_{0.5}O_4$

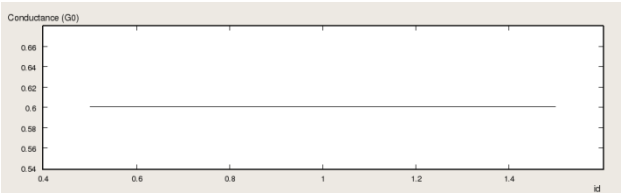

Fig. 5 – Conductance of $LiMn_{1.5}Ni_{0.5}O_4$

Table 4 – Total energy calculations of $LiMn_{1.5}Ni_{0.5}O_4$

Energy component	Before Optimization	After Optimization
External-field	0.0000 eV	8.23106 eV
Exchange Correlation	– 2172.4484 eV	– 4331.82060 eV
Electrostatic	8279.86396 eV	16846.7571 eV
Kinetic	4496.76739 eV	9083.24743 eV
Total Energy	5955.60544 eV	12176.29857 eV

The band structure of intercalation compounds has been studied extensively with electronic structure methods. In this rigid band picture, Li intercalation causes the Fermi level to rise, and intercalation curve, the variation of the voltage with the Li content of the cathode, hence reflects the shape of the density of states at the Fermi level. In this rigid-band model, the Fermi level remains unchanged as Li is intercalated, but the density of states translates to lower energies. Computed band structure of $LiMn_{1.5}Ni_{0.5}O_4$ experimentally determined lattice parameters and found that the bands derived from the metal s orbital shifted upon intercalation of lithium. Attempts to obtain intercalation voltages with first principles calculations are limited and have focused on band structure of the material .To examine the splitting of the energy bands, we calculated the change in electronic energy [23].

The electronic density of states (DOS) are plotted for $LiMn_{1.5}Ni_{0.5}O_4$ shown in Fig. 5. By computing the total energy of a lithiated compound it is possible to predict average intercalation voltage for Li. The fact that metastable structures may be used for the intercalation compounds in rechargeable batteries they operate near room temperatures [24]. As demonstrated in this paper , first-principles methods can be used to predict the average intercalation voltage in given structure with high accuracy.The capability of predicting intercalation voltages without the need for experimental data also allowed us to systematically investigate the effect of metal,cation,and structure,by computing the intercalation voltage for many structures [25].

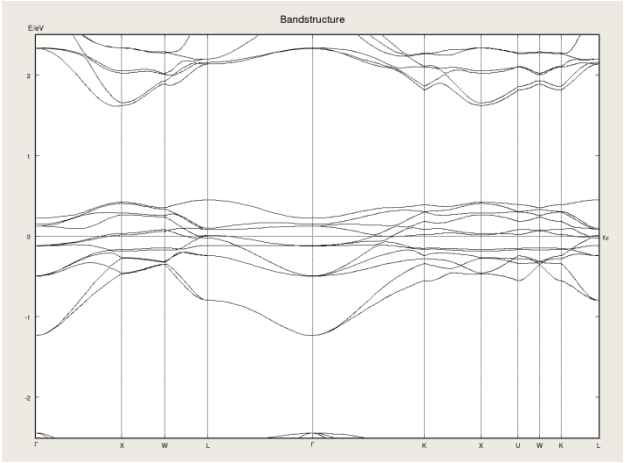

Fig. 6 – Band structure of spinel $LiMn_{1.5}Ni_{0.5}O_4$

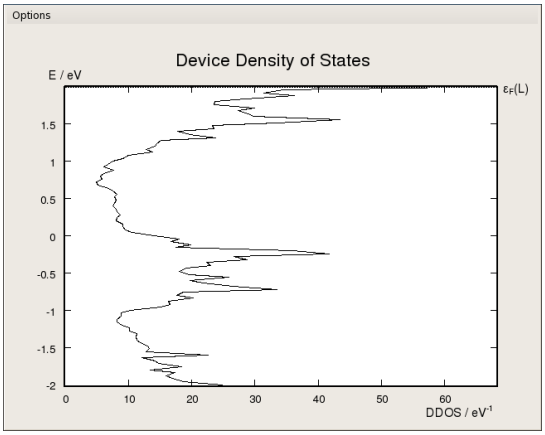

Fig. 7 – Density of states of spinel $LiMn_{1.5}Ni_{0.5}O_4$

4. CONCLUSION

The electro active nano $LiMn_{1.5}Ni_{0.5}O_4$ spinel has been synthesized by co-precipitation chemical method with subsequent calcination at 700 °C for 6 h. Powder X-ray diffraction analysis shows that the sample is pure single phase and good crystallization. We have demonstrated achievements in predicting structural and electronic properties of $LiMn_{1.5}Ni_{0.5}O_4$ using DFT based first principle methods. These capabilities establish first principle computation as an invaluable tool in the design of electrode material at nano scale for Lithium ion battery.

REFERENCES

1. J. Molenda, *Material Problems and Prospects Of Li-ion Batteries for vehicles applications. World scientific* (2011).
2. M.M. Abou-Sekkina, K.M. Elsabawy, F.G. Elmetwaly, *Narrow Range of Y^{+++}-Dopings on $LiM_{2-x}Mn_xO_4$ for promoting structural, Microstructural and cathodic capacity features of LiMnO- spinel* (PRL-2010).
3. F. Espinosa-Mangana, L. Alvarez-contreras, O. Morales-Rivera, M.T. Ochoa-Lara, S.M. Loya-mancilla, A. Aguilar-Eluguezabal, *Electron energy-loss spectroscopy of $LiMn_2O_4$, $LiMn_{1.6}Ti_{0.6}O_4$ and $LiMn_{1.5}Ni_{0.5}O_4$* (Elsevier: 2008).
4. K. Yamaura, Q. Huang, L. Zhang, K. Takada, Y. Baba, T. Nagai, Y. Matsui, K. Kosuda, E.T. Muromachi, *Spinel-to-$CaFe_2O_4$ Type structural transformation in $LiMn_2O_4$ under high pressure*.
5. M. Faraz, K.V. Rao, Y. Aparna, *Synthesis and Charecterizationof $LiMn_{1.5}Ni_{0.5}O_4$ Nanoparticles by Solution Combustion Method* (ASP-2012).
6. J. Akimoto, Y. Takahashi, Y. Gotoh, S. Mizuta, *J. Crystal Growth* **229**, 405 (2001).
7. M. Lauer, R. Valenti, H.C. Kandpal, R. Sheshadri, *Phys. Rev. B* **69**, 075117 (2004).
8. N.N. Shukla, S. Shukla, R. Prasad, R. Benedek, *Modelling Simul. Mater.Sci. Eng.* **16**, 055008 (2008)
9. R. Dreizler, E. Gross, *Density Functional Theory* (Plenum Press: New York: 1990).
10. L. Wang, T. Maxisch, G. Ceder, *Phys. Rev. B* **73**, 195107 (2006).
11. S.T. Myung, H.T. Chung, S. Komaba, N. Kumagai, *J. Power Sources* 90, 103 (2000).
12. M.D. Levi, K. Gamolsky, D. Aurbach, U. Heider, R. Oesten, *J. Electrochem. Soc.* **147**(1), 25 (2000).
13. D. Morgan, G. Ceder, M.Y. Saidi, J. Barker, J. Swoyer, H. Huang, G. Adamson, *J. Power Sources* 119, 755 (2003).
14. A.V. Ven, C. Marianetti, D. Morganand, G. Ceder, *Solid State Ionics* **135**, 21 (2000).
15. A.V. Venand, G. Ceder, *Phys. Rev. B* **59**, 742 (1999).
16. J. Wolfenstineand, J. Allen, *J. Power Sources* **142**, 389 (2005).
17. H. Jonsson, G. Mills, K.W. Jacobsen, *Nudged Elastic Band Method for Finding Minimum Energy Paths of Transitions* (Ed. by B.J. Berne, G. Ciccotti, D.F. Coker) (World Scientific Publishing Company: RiverEdge, NJ: 1998).
18. C.S. Chaubey, Kim, *J. Bull. Korean Chem. Soc.* **12**, 2279 (2007).
19. J.S. Jung, L. Malkinski, J.H. Lim, M. Yu, C.J. O'Connor, H.O. Lee, E.M. Kim, *Bull. Korean Chem. Soc.* **29**, 758 (2008).
20. B. Gillot, *Eur. Phys. J. Appl. Phys.* **4**, 243 (1998).
21. M. Sugimoto, *J. Am. Ceram. Soc.* **82**, 269 (1999).
22. Z.X. Tang, C.M. Sorensen, K.J. Klabunde, G.C. Hadjipanayis, *Phys. Rev. Lett.* **67**, 3602 (1991).
23. G.U. Kulkarni, K.R. Kannan, T. Arunarkavalli, C.N.R. Rao, *Phys. Rev. B* **49**, 724 (1994).
24. P.J. Zaag, V.A. Brabers, M.T. Johnson, A. Noord-er-meer, P.E. Bongers, *Phys. Rev. B* **51**, 12009 (1995).
25. T. Roisnel, Rodriguez-Carvajal, J. *WINPLOTR, a New Tool forPowder Diffraction*. Laboratoire Leon.